ISSN 1063-7761, Journal of Experimental and Theoretical Physics, 2012, Vol. 114, No. 5, pp. 841–849. © Pleiades Publishing, Inc., 2012.
Original Russian Text © V.A. Dudnikov, S.G. Ovchinnikov, Yu.S. Orlov, N.V. Kazak, C.R. Michel, G.S. Patrin, G.Yu. Yurkin, 2012, published in Zhurnal Eksperimental'noi i Teoreticheskoi Fiziki, 2012, Vol. 141, No. 5, pp. 966–975.

ELECTRONIC PROPERTIES OF SOLID

# Contribution of $Co^{3+}$ Ions to the High-Temperature Magnetic and Electrical Properties of $GdCoO_3$

**V. A. Dudnikov[a,b,*], S. G. Ovchinnikov[a,c], Yu. S. Orlov[a], N. V. Kazak[a], C. R. Michel[d], G. S. Patrin[a,c], and G. Yu. Yurkin[a]**

[a] *Kirensky Institute of Physics, Siberian Branch, Russian Academy of Sciences, Akademgorodok 50–38, Krasnoyarsk, 660036 Russia*
**e-mail: slad63@yandex.ru*
[b] *Reshetnev Siberian State Aerospace University, pr. im. Gazety "Krasnoyarskii Rabochii" 31, Krasnoyarsk, 660014 Russia*
[c] *Siberian Federal University, Krasnoyarsk, 660041 Russia*
[d] *Universidade de Guadalajara, Guadalajara, 44430 Mexico*

Received July 5, 2011

**Abstract**—The temperature dependence of the static magnetization of polycrystalline rare-earth cobaltite $GdCoO_3$ is measured in the temperature range 2–800 K. The magnetic behaviors of $GdCoO_3$ and $Gd^{3+}$ are found to be different at temperatures above room temperature, which is caused by the appearance of a contribution from $Co^{3+}$ ions at high temperatures. The temperature dependence of the magnetic susceptibility of $GdCoO_3$ is determined by the magnetization of rare-earth gadolinium ions and the additional paramagnetic contribution induced by the thermally excited magnetic terms of $Co^{3+}$ ions. The LDA + GTB method is used to calculate the electronic structure of $GdCoO_3$ in the temperature range 0–300 K with allowance for strong electron correlations. The energy spectrum of $GdCoO_3$ is found to have intragap states that decrease the dielectric gap width with increasing temperature.

**DOI:** 10.1134/S106377611203003X

## 1. INTRODUCTION

The family of perovskite-like cobaltites has a wide set of properties inherent in other 3*d* metal oxides, namely, superconductivity, metal–insulator transitions, colossal magnetoresistance, and the interrelation between the charge, spin, and orbit degrees of freedom that is common for all strong electron correlation (SEC) systems [1]. However, cobaltites have a specific spin crossover property, i.e., the inversion of the high- and low-spin terms of the $Co^{3+}$ ion in the ground state. Such crossovers are also known for oxides with $Fe^{3+}$ and $Mn^{2+}$ ions at high pressures. The energy of the low-spin (LS) term in the ground state of $LaCoO_3$ lies below the nearest excited level by spin gap $\Delta_{s-t} \approx 150$ K [2]. When the temperature increases, a diffuse phase transition from a diamagnetic to a paramagnetic insulator takes place at temperature $T \sim \Delta_{s-t}$. The gap in rare-earth $LnCoO_3$ cobaltites is larger due to lanthanide compression. Neutron scattering data [3, 4] showed the absence of spin transitions at temperatures up to room temperature in cobaltites with Ln = Pr, Nd, Sm, and Eu. The structural anomalies that accompany the spin transition in $LnCoO_3$ (Ln = Y, Sm, Dy, Gd) compounds are observed at temperatures much higher than room temperature [5]. Therefore, the contribution of $Co^{3+}$ ions to the magnetic properties is absent in the standard temperature range from room to lower temperatures. In the case of $GdCoO_3$, $Gd^{3+}$ ions have $S = 7/2$ and provide paramagnetic properties. At $T < 3.3$ K, antiferromagnetic ordering of gadolinium spins was detected [6].

The purpose of this work is to study the magnetic and electrical properties of $GdCoO_3$ at high temperatures. To this end, we measure the magnetization over a wide temperature range. When subtracting the paramagnetic contribution of gadolinium from these data, we find the contribution of $Co^{3+}$, which increases with temperature. We then simulate this contribution using the multielectron LDA + GTB method, which was recently used to calculate the magnetic and electrical properties of $LaCoO_3$ [7], and find spin gap $\Delta_{s-t}$ for $GdCoO_3$. Using this gap, we calculate the electronic structure and its temperature dependence, which is caused by the population of high-spin states with increasing temperature. As a result, the dielectric gap decreases by an order of magnitude at $T = 300$ K as compared to zero temperature.

The structure of this work is as follows. In Section 2, we describe samples and measurement techniques. In Section 3, we present magnetic data and separate the contribution of cobalt. In Section 4, we calculate the magnetic contribution of $Co^{3+}$ ions with allowance for low- and high-spin states and determine the spin gap. In Section 5, the temperature-dependent band structure of the Hubbard fermions in $GdCoO_3$ is calculated by the LDA + GTB method, and the results are discussed in Section 6.

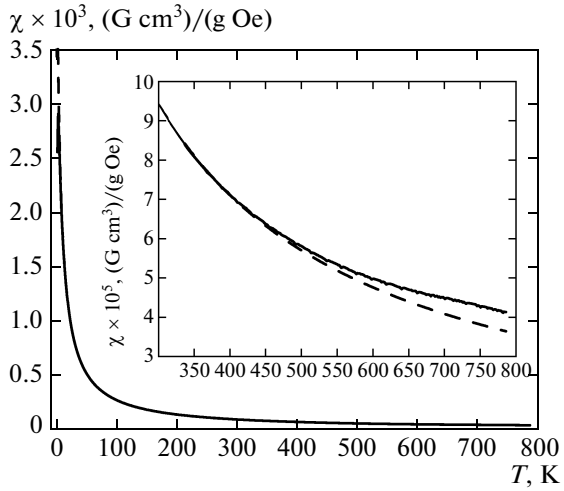


**Fig. 1.** Temperature dependences of (solid curve) $GdCoO_3$ and (dashed curve) $Gd^{3+}$ in a field of 5 kOe. (inset) High-temperature measurement range that shows an increase in the contribution of $Co^{3+}$ ions with the temperature.

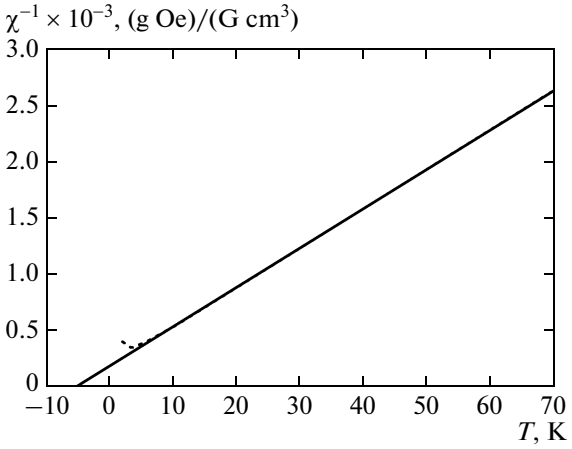


**Fig. 2.** Temperature dependence of reciprocal magnetic susceptibility $1/\chi(T)$ of $GdCoO_3$. (dotted curve) Approximation by the Curie–Weiss law at a Curie temperature $\Theta = -5.3$ K (straight line).

## 2. EXPERIMENTAL

Polycrystalline $GdCoO_3$ samples were prepared by the solution sol gel method [8], in which stoichiometric amounts of cobalt and gadolinium nitrates were dissolved in deionized water and then were dried at a temperature of 90°C for 6 h. The powder thus prepared was annealed at a temperature of 300°C in air, pressed into pellets 12 mm in diameter, and subjected to repeat annealing. We measured the temperature dependences of static magnetization in the temperature range from 2 to 800 K in a magnetic field of 5 kOe. The measurements were performed on an MPMS-XL Quantum Design SQUID magnetometer. The relative measurement error was $\Delta\chi/\chi \le 0.01$, so that the error ($\Delta\chi \sim 10^{-6}$) for a measured magnetic susceptibility of $\chi \sim 10^{-4}$ is smaller than the line width in the experimental curves. The crystal structure of the samples was studied in [9] using a DRON-4 diffractometer at room temperature.

## 3. EXPERIMENTAL RESULTS

Comprehensive investigations of the magnetic and electrical properties of $GdCoO_3$ in the temperature range 4.2–300 K were considered in [9, 10]. It was found that the behavior of $GdCoO_3$ in this temperature range is close to the behavior of a set of free $Gd^{3+}$ ions. At $T < 4.2$ K, $GdCoO_3$ exhibits antiferromagnetic properties and behaves as an antiferromagnet with a Néel temperature $T_N = 3.3$ K [6].

The solid line in Fig. 1 shows the temperature dependence of the magnetic susceptibility $\chi(T)$ of $GdCoO_3$ in the temperature range 2–800 K and a magnetic field $H = 5$ kOe. At low temperatures, the magnetic susceptibility is seen to increase substantially. At $T > T_N$, the $\chi(T)$ dependence is monotonic and has no specific features. The temperature dependence of the reciprocal magnetic susceptibility is well approximated by a straight line (Fig. 2), which can be used to determine the asymptotic Curie temperature ($\Theta = -5.3$ K).

We compare the experimental magnetic susceptibility curve $\chi(T)$ obtained for $GdCoO_3$ with the graphical $\chi(T)$ dependence obtained for free $Gd^{3+}$ ions presented in Fig. 1 and calculated by the formula [11]

$$\chi = \frac{g_J^2 \mu_B^2 J(J+1)N}{3k(T-\theta)}, \qquad (1)$$

where $N$ is the number of $Gd^{3+}$ ions per unit volume, $\mu_B$ is the Bohr magneton, $k_B$ is the Boltzmann constant, $J = S = 7/2$, and $g_J = 2$, and revealed a difference between the experimental and calculated results when the temperature increases. Obviously, a contribution from $Co^{3+}$ ions appears in the magnetic susceptibility of $GdCoO_3$ when the temperature increases. When subtracting the paramagnetic contribution of $Gd^{3+}$ ions from the experimental data, we can determine the contribution of $Co^{3+}$ ions. The contribution of $Co^{3+}$ ions to the magnetic susceptibility of $GdCoO_3$ is seen to increase with temperature (Fig. 1, inset).

## 4. MAGNETIC PROPERTIES OF $Co^{3+}$ IONS WITH ALLOWANCE FOR LOW- AND HIGH-SPIN STATES

The total magnetization of $GdCoO_3$ can be presented as the sum of two independent terms, $M_{GdCoO_3} = M_{Gd} + M_{Co}$, where $M_{Gd}$ and $M_{Co}$ are the magnetizations of gadolinium and cobalt ions, respectively. To describe the contribution of $Co^{3+}$ ions to the total magnetization of $GdCoO_3$, we consider the energy

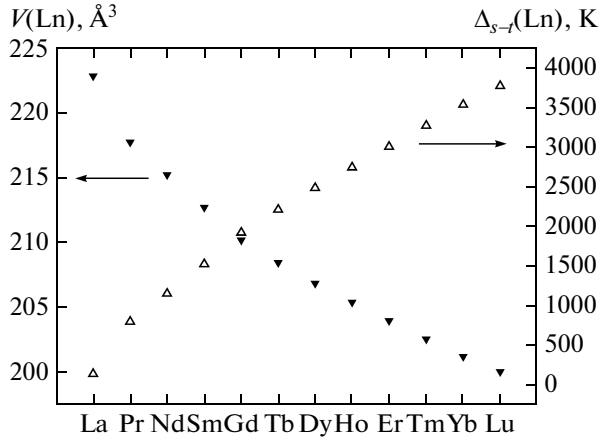


**Fig. 3.** (dark triangles) Unit cell volume of cobaltite $LnCoO_3$ $V$(Ln) vs. the rare-earth ion substituting for lanthanum and (light triangles) the same dependence for spin gap $\Delta_{s-t}$.

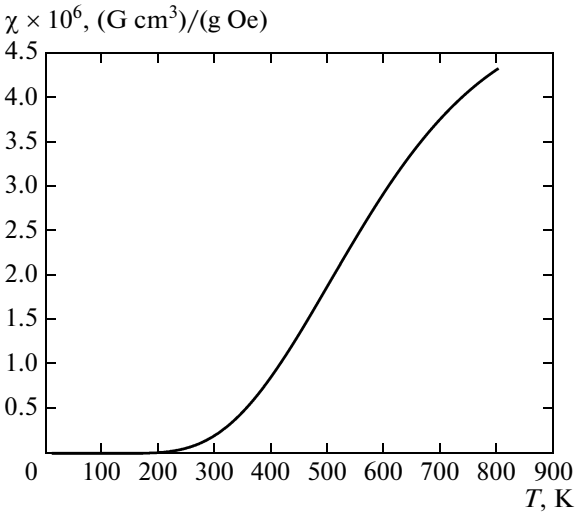


**Fig. 4.** Magnetic susceptibility of $Co^{3+}$ ions with a spin gap $\Delta_{s-t} = 2000$ K.

levels of $Co^{3+}$ ions in the crystal field allowing for the spin–orbit interaction (Fig. 6b). The ground term is represented by low-spin singlet $^1A_1$ separated from triplet sublevel $\tilde{J} = 1$ of high-spin state $^5T_2$ by spin gap $\Delta_{s-t}$. At $\Delta_{s-t} = 150$ K, the term positions correspond to the data obtained for $LaCoO_3$ in [2, 12, 13]. The substitution of a certain rare-earth ion with a smaller ionic radius for lanthanum leads to the appearance of chemical pressure, which is equivalent to an external pressure. This pressure is caused by the record compressibility of the Co–O bond in cobalt–oxide compounds [16]. Therefore, this substitution results in additional stabilization of a low-spin state, in other words, in an increase in the spin gap. The value of $\Delta_{s-t}$ for $GdCoO_3$ at low temperatures can be found from the following considerations.

Spin gap $\Delta_{s-t}$ is determined as the difference between the energies of high-spin (HS) and low-spin states, which can be represented in terms of the intraionic Racah (Coulomb interaction) parameters and crystal field $\Delta = 10$ Dq. The Racah parameters for $Co^{3+}$ in $LaCoO_3$ and $GdCoO_3$ are assumed to be the same; then, the dependence of $\Delta_{s-t}$ on the interatomic distance is $2\Delta$ : $\Delta_{s-t} = \Delta_{at} + 2\Delta$, where $\Delta_{at}$ is the gap determined by the intraionic Coulomb interaction energy. As a result of lanthanide compression, parameter $\Delta$ is different for $LaCoO_3$ and $GdCoO_3$; then, we can write

$$\Delta_{s-t}(\mathrm{Gd}) = \Delta_{s-t}(\mathrm{La}) + 2(\Delta(\mathrm{Gd}) - \Delta(\mathrm{La})). \quad (2)$$

Additional chemical pressure $P$ induced by lanthanide compression can be determined from the Birch–Murnaghan equation [14, 15]

$$P(V) = \frac{3}{2}B_0\left[\left(\frac{V_0}{V}\right)^{7/3} - \left(\frac{V_0}{V}\right)^{5/3}\right] \times \left\{1 + \frac{3}{4}(B_0' - 4)\left[\left(\frac{V_0}{V}\right)^{2/3} - 1\right]\right\}, \quad (3)$$

where $B_0$ and $B_0'$ are the empirical parameters having the meaning of the isothermal modulus of dilatation and its first pressure derivative (for $LaCoO_3$, $B_0 =$ 150 GPa, $B_0' = 4$ [16]), respectively; $V_0$ is the unit cell

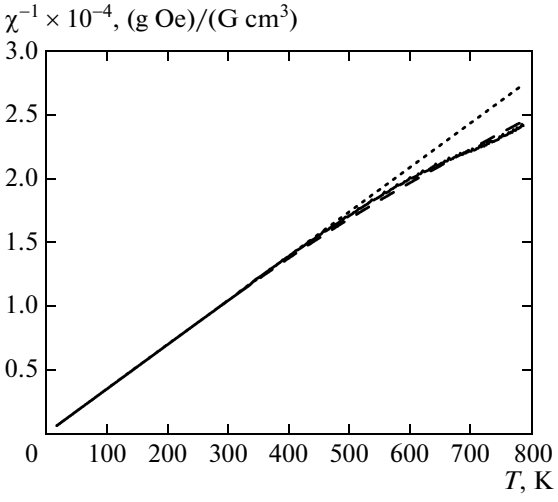


**Fig. 5.** Temperature dependence of the reciprocal magnetic susceptibility. (solid line) Experimental data for $GdCoO_3$, (dotted line) Curie–Weiss magnetic susceptibility of gadolinium ions, and (dashed line) calculated magnetic susceptibility of gadolinium and cobalt.

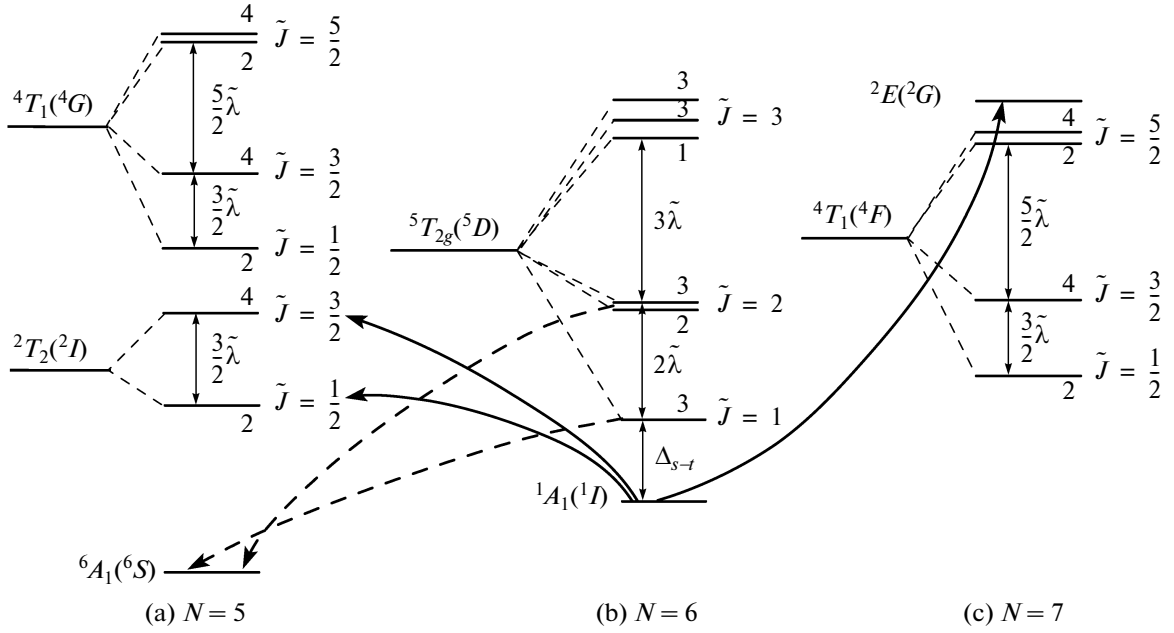


**Fig. 6.** Set of low-energy terms for electronic configurations (a) $d^5$, (b) $d^6$, and (c) $d^7$ in the crystal field. At $T = 0$, only ground low-spin singlet $^1A_1$ ($N = 6$) is populated; Fermi excitations forming the conduction band bottom and the valence band top are shown by solid lines. The dashed lines indicate the transitions responsible for the formation of intragap states upon an increase in the temperature. Their spectral weight is determined by the population of the high-spin state of the $d^6$ configuration.

volume of $LaCoO_3$; and $V$ is the unit cell volume for lanthanide Ln. For $LaCoO_3$, we have $V_0 = 222.83$ Å$^3$; for $GdCoO_3$, $V = 210.2$ Å$^3$; therefore, $P = 9.81$ GPa. Lattice compression increases the crystal field, which can be represented as

$$\Delta(P) = \Delta(0) + \alpha_\Delta P. \quad (4)$$

Baric derivative $\alpha_\Delta$ can be considered as an empirical parameter. This parameter has recently been determined by studying the spin crossover (transition from a high-spin into a low-spin state) in magnesiowustite $Mg_{0.75}Fe_{0.25}O$, which has a similar type of chemical bond and a similar electronic structure formation mechanism [17]. For estimation, we assume that $\alpha_\Delta$ for $GdCoO_3$ is the same, i.e., $\alpha_\Delta = 0.0078$ eV/GPa. Then, the spin gap in $GdCoO_3$ is $\Delta_{s-t} \approx 2000$ K. The spin gap can also be estimated for other lanthanides from their unit cell volumes (Fig. 3).

At low temperatures, the cobalt ions in $GdCoO_3$ exist in nonmagnetic LS state $^1A_1$. When the temperature increases, an HS state with a nonzero magnetic moment is thermally excited and the magnetization increases. The statistical sum of $Co^{3+}$ ions of one mole of $GdCoO_3$ takes the form

$$Z = [1 + e^{-\beta\Delta_{s-t}} + e^{-\beta\Delta_{s-t}} \times 2\cosh(g\mu_B\tilde{B}\beta) + e^{-\beta(\Delta_{s-t}+2\tilde{\lambda})} + e^{-\beta(\Delta_{s-t}+2\tilde{\lambda})} \times 2\cosh(g'\mu_B\tilde{B}\beta) + e^{-\beta(\Delta_{s-t}+2\tilde{\lambda})} \times 2\cosh(g''\mu_B\tilde{B}\beta)]^{N_A}, \quad (5)$$

where $\tilde{\lambda}$ is the effective spin–orbit interaction constant, $N_A$ is Avogadro's number, $\tilde{B}$ is the applied magnetic field, $k_B$ is the Boltzmann constant, $\beta = 1/k_BT$, and $\mu_B$ is the Bohr magneton. The Lande factors are $g = 3.4$ for triplet $\tilde{J} = 1$ and $g' = 3.1$ and $g'' = 1.8$ for quintet $\tilde{J} = 2$. Knowing the statistical sum, we can find the free energy $F = -k_BT\ln Z$ and the magnetization $M = -\partial F/\partial\tilde{B} = k_BT \cdot 1/Z \cdot \partial Z/\partial\tilde{B}$ in a standard manner. For not very low temperatures and not very high magnetic fields at $g\mu_B\tilde{B}\beta \ll 1$, the expression $\chi_{Co} = \partial M/\partial\tilde{B}$ for the molar magnetic susceptibility of $Co^{3+}$ ions takes the form

$$\chi_{Co} = N_A 2\mu_B^2\beta[g_1^2 e^{-\beta\Delta_{s-t}} + g'^2 e^{-\beta(\Delta_{s-t}+2\tilde{\lambda})} + g''^2 e^{-\beta(\Delta_{s-t}+2\tilde{\lambda})}][1 + 3e^{-\beta\Delta_{s-t}} + 5e^{-\beta(\Delta_{s-t}+2\tilde{\lambda})}]^{-1}. \quad (6)$$

The solid line in Fig. 4 shows the results of calculating $\chi_{Co}$ at $\tilde{\lambda} = 185$ K [12] and $\Delta_{s-t} = 2000$ K.

The solid line in Fig. 5 shows the experimental behavior of the temperature dependence of the reciprocal magnetic susceptibility of $GdCoO_3$, $1/\chi_{GdCoO_3}$. For comparison, the dotted line shows the behavior of the reciprocal magnetic susceptibility of gadolinium, $1/\chi_{Gd}$ (see Eq. (1)), and the dashed line illustrates the

calculation results for the total reciprocal magnetic susceptibility of gadolinium and cobalt, $1/(\chi_{Gd} + \chi_{Co})$. The calculated curve is seen to describe the general dependence and the deviation of the experimental data from the paramagnetic susceptibility of gadolinium, which is related to the additional contribution of cobalt ions to the magnetization of $GdCoO_3$.

## 5. TEMPERATURE DEPENDENCE OF THE ELECTRONIC STRUCTURE OF $GdCoO_3$

One of the interesting specific features of perovskite-like rare-earth $LnCoO_3$ cobaltites (where Ln stands for La or lanthanide Pr, Nd, Sm, Eu, Gd, Tb, Ho) is a smooth insulator–metal transition occurring when the temperature increases. The electron phase diagram of $LnCoO_3$ with a rare-earth ion ranging from La to Lu has the following three characteristic regions: nonmagnetic insulator, paramagnetic insulator, and paramagnetic metal [18]. The transitions between them are smooth and diffuse: these are crossovers rather than classic phase transitions. The characteristic temperature of transition into a metallic state $T_{IMT}$ shifts toward high temperatures when La is replaced by a rare-earth ion with a smaller ionic radius. For example, we have $T_{IMT} \approx 550$ K for $LaCoO_3$ and $T_{IMT}$ is more than 1000 K for $GdCoO_3$. As noted above, the introduction of an element with a different ionic radius in a crystal lattice causes chemical pressure, which acts similarly to an external pressure. Therefore, if the ionic radius of this element is smaller than that of the rare-earth ion of the initial compound, such a replacement causes additional stabilization of a low-spin state, i.e., increases $\Delta_{s-t}$. This is also true of partial substitution. For example, the dielectric properties of compound $La_{1-x}Eu_xCoO_3$ are more pronounced and retained for a longer time as the temperature increases when La is replaced by the Eu ion with a smaller ionic radius and concentration $x$ increases [19].

The nature of the dielectric state in rare-earth cobaltites is clear. As in all oxides of transition metals, the presence of a dielectric gap is caused by strong electron–electron interactions of the $3d$ ion of a transition metal. However, the substantial difference between spin gap $\Delta_{s-t}$ and activation energy $E_a$ of electrical conductivity at low temperatures implies that $LnCoO_3$ compounds are not simple band insulators [20]. For example, the basic representative of this row ($LaCoO_3$) is characterized by $\Delta_{s-t} \approx 150$ K and $E_a \approx 0.1$ eV. Moreover, a considerable difference between charge gap $2E_a$ and insulator–metal transition temperature $T_{IMT}$ indicates that the latter can hardly be explained by the model of a narrow-gap semiconductor [21]. For example, for $LaCoO_3$ we have $2E_a \approx 2300$ K and $T_{IMT} \approx 550$ K.

As noted above, $GdCoO_3$ (as most oxides of transition metals) is a system with strong electron correlations, which create difficulties for their theoretical description and play an important role in the formation of various properties of these materials. The traditional one-electron approaches cannot describe many of them; in addition, it becomes apparent that the description of these properties should take into account the intimate relationship between the charge, orbit, spin, and lattice degrees of freedom. Therefore, adequate methods should be used to describe the electronic structures of such compounds. One of these methods is represented by the generalized tight binding (GTB) method [22], which is the implementation of Hubbard's ideas for multielectron and multiorbital systems, and its ab initio version LDA + GTB [23]. The LDA + GTB method combines LDA band calculations, which are used to calculate the Wannier functions, the tight binding Hamiltonian parameters, and the parameters of the Coulomb $U$ and Hund exchange $J$ interactions, with the GTB scheme. The GTB method is a version of the cluster perturbation theory and uses an exact diagonalization of a multielectron Hamiltonian inside a unit cell and the theory of perturbation with respect to the parameter of effective hopping between unit cells.

We write the Hamiltonian of a multiband $p$–$d$ model in the form

$$H = H_d + H_p + H_{pd}^{\text{hop}} + H_{pp}^{\text{hop}} + H_{dd}^{\text{coul}}. \quad (7)$$

Here, the first two terms are responsible for the local one-electron energies of cation electrons in the crystal field and anion $p$ electrons, and the third term is $p$–$d$ hopping (hybridization) Hamiltonian $t_{pd}$. Term $H_{pp}^{\text{hop}}$ is related to oxygen–oxygen hopping $t_{pp}$, and $H_{dd}^{\text{coul}}$ is the energy of the electrostatic interaction of the electrons of a transition-metal ion. To take into account $p$–$d$ hybridization and strong electron correlations, we divide a lattice into nonintersecting clusters (cells). The Hamiltonian of a multiband $p$–$d$ model is written as

$$H = H_0 + H_1,$$
$$H_0 = \sum_f H_c(f), \quad H_1 = \sum_{f,g} H_{cc}(f,g), \quad (8)$$

where $H_c(f)$ is the intracellular part of Hamiltonian $H$ and $H_{cc}(f, g)$ describes the hopping and interaction between the $f$th and $g$th cells. Using a numerical diagonalization of intracellular part $H_c(f)$, we find multielectron eigenstates $|m, N\rangle \equiv |p\rangle$ for various subspaces of the Hilbert space labeled by number $N$ of electrons in a cell.

The $X$ operator at site $f$ is defined as

$$X_f^{pq} = |p\rangle\langle q| = |m, N\rangle\langle m', N'|. \quad (9)$$

We assume that eigenstates $|p\rangle$ of neighboring cells are orthogonal. Otherwise (as in the case of cobaltites, where two neighboring $CoO_6$ clusters contain a common oxygen atom), an orthogonalization procedure should be used; that is, we have to construct a Wannier

function in an explicit form instead of group oxygen orbitals. Such a procedure was first proposed for a three-band $p$–$d$ model [24] and was then generalized to a multiband model [25].

In the standard notation of $X$ operators, we are dealing with cumbersome and awkward notation for the initial and final states. To simplify this notation, we will employ Zaitsev's idea [26] and introduce so-called root vector $(p, q) \longleftrightarrow \alpha(p, q) \equiv \alpha$ instead of a pair of indices $(p, q)$. Moreover, since the set of such vectors is countable, we will label each of these vectors as $\alpha \longleftrightarrow \alpha_n$ and will only indicate root vector number $n$

$$X_f^{pq} \longleftrightarrow X_f^{\alpha(p,q)} \longleftrightarrow X_f^{\alpha_n} \longleftrightarrow X_f^n. \tag{10}$$

We define vectors $\alpha$ so that they correspond to electron annihilation (i.e., $N_q - N_p = +1$). Then the annihilation (production) operators for an electron in state $|f\lambda\sigma\rangle$ can be exactly written in the $X$ representation in the form

$$\begin{aligned} a_{f\lambda\sigma} &= \sum_n \gamma_{\lambda\sigma}(n) X_f^n, \\ a_{f\lambda\sigma}^\dagger &= \sum_n \gamma_{\lambda\sigma}^*(n) (X_f^n)^\dagger, \\ \gamma_{\lambda\sigma}(n) &= \langle p | a_{f\lambda\sigma} | q \rangle. \end{aligned} \tag{11}$$

Subscript $\lambda$ runs through the entire set of the electron orbitals $(p, d)$, and subscript $\sigma$ runs two spin projections.

In the $X$ operator representation, the total Hamiltonian takes the form

$$H_{pq} = \sum_{f,p} E_p X_f^{pp} + \sum_{f \neq g} \sum_{nn'} \tilde{t}_{fg}^{nn'} X_f^{\dagger n} X_g^{n'}, \tag{12}$$

where $\tilde{t}_{fg}^{nn'} = \sum_{\lambda\lambda'} \tilde{t}_{fg}^{\lambda\lambda'} \gamma_{\lambda\sigma}^*(n) \gamma_{\lambda'\sigma}(n')$ and $\tilde{t}_{fg}^{\lambda\lambda'}$ are the effective intercellular hopping parameters (i.e., the hopping matrix elements of the initial Hamiltonian renormalized upon orthogonalizaiton).

The obvious similarity between Eq. (12) and the Hubbard model Hamiltonian allows us to use many methods of the perturbation theory in parameter $\tilde{t}/U_{\text{eff}}$ that are known for the Hubbard model ($U_{\text{eff}} = E(d^{n+1}) + E(d^{n-1}) - 2E(d^n)$ is the effective Hubbard energy).

In the $X$ operator diagram technique [27, 28], perturbation theory series are constructed not for the electron Green's function

$$G_{k\sigma}^{\lambda\lambda'}(\omega) = \langle\langle a_{k\lambda\sigma} | a_{k\lambda'\sigma}^\dagger \rangle\rangle_\omega,$$

but for matrix Green's function

$$D_k^{nn'}(\omega) = \langle\langle X_k^n | (X_k^{n'})^\dagger \rangle\rangle_\omega;$$

these two functions are connected by the equality

$$G_{k\sigma}^{\lambda\lambda'}(\omega) = \sum_{n,n'} \gamma_{\lambda\sigma}(n) \gamma_{\lambda'\sigma}^*(n') D_k^{nn'}(\omega) \tag{13}$$

due to Eq. (11).

Since Hamiltonian $H_c$ in the Hubbard operator representation has a diagonal form, local Green's function can be calculated directly by the expression

$$G_{(0)\sigma}^{\lambda\lambda'}(\omega) = \sum_n |\gamma_{\lambda\sigma}(n)|^2 \delta_{\lambda\lambda'} \frac{F(n)}{\omega - \Omega_n + i\delta}, \tag{14}$$

where $\Omega_n = E_{m'}(N+1) - E_m(N)$ and the filling factor is $F(n) = \langle X_f^{pp} \rangle + \langle X_f^{qq} \rangle$.

Obviously, Green's function (14) implements the Lehman representation in a unit cell. All quantities appearing in Eq. (14) are calculated in terms of the local characteristics of terms and multielectron states $|m, N\rangle$. In our case for $GdCoO_3$, low terms with $N = 5$, 6, and 7, which correspond to electron configurations $d^5$, $d^6$, and $d^7$, respectively, of the cobalt ion in the crystal field, are important. Here, index $n$ denotes quasiparticles with charge $e$, a spin of 1/2, energy $\Omega_n$, and spectral weight $A_{\lambda\sigma}(n) = |\gamma_{\lambda\sigma}(n)|^2 F(n)$. At the same time, the total spectral weight is preserved in the same way as for free electrons due to the completeness of the basis of multielectron states $|p\rangle$.

The spectral density of one-particle excitations can be expressed in terms of Fermi one-particle Green's function

$$\begin{aligned} A_\sigma(k, \omega) &= -\frac{1}{\pi} \sum_{\lambda, n, n'} \gamma_{\lambda\sigma}(n) \gamma_{\lambda\sigma}^*(n') \\ &\times \operatorname{Im} D_k^{nn'}(\omega + i\delta) \\ &= -\frac{1}{\pi} \sum_\lambda \operatorname{Im} G_{k\sigma}^{\lambda\lambda}(\omega + i\delta) \end{aligned} \tag{15}$$

and the density of one-particle states for a given spin projection ($N_k$ is the normalization factor)

$$N_\sigma(\omega) = \frac{1}{N_k} \sum_k A_\sigma(k, \omega). \tag{16}$$

For Green's function $\hat{D}$, we can write the generalized Dyson equation [27]

$$\begin{aligned} \hat{D}_k(\omega) = \{ &(\omega - \Omega_n)\delta_{nn'} \\ &- \hat{P}_k(\omega) \hat{\tilde{t}}(k) - \hat{\Sigma}_k(\omega) \}^{-1} \hat{P}_k(\omega). \end{aligned} \tag{17}$$

Here, $\hat{\Sigma}_k(\omega)$ and $\hat{P}_k(\omega)$ are the mass and force operators, respectively. The presence of the force operator, which is called the end factor in the $X$ operator diagram technique [26], is associated with a spectral weight redistribution and is a fundamental SEC effect.

In the Hubbard I approximation, the structure of exact Green's function (17) is preserved, but the mass

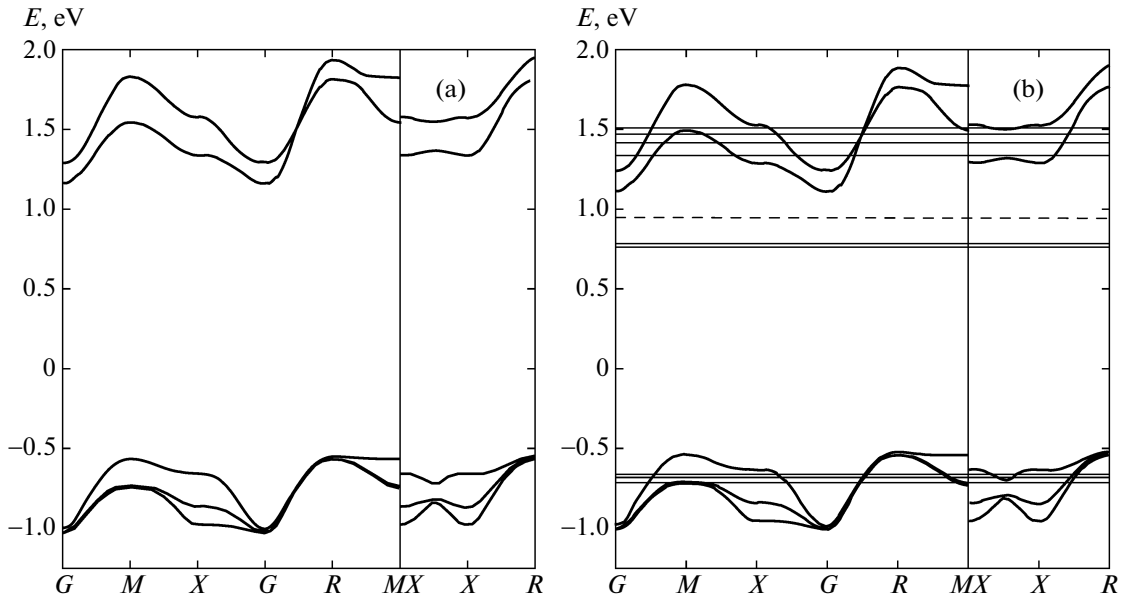


**Fig. 7.** Quasiparticle spectrum for $T =$ (a) 0 and (b) 300 K. $G(0, 0, 0)$, $M(\pi, \pi, 0)$, $X(\pi, 0, 0)/(0, \pi, 0)$, and $R(\pi, \pi, \pi)$ are symmetric points in the Brillouin zone. At finite temperatures, new bands appear both inside the gap and the valence and conduction bands, and these bands decrease the dielectric gap energy from $E = 1.7$ eV at $T = 0$ K to $E = 0.4$ eV at $T = 300$ K.

operator is set at zero and the force operator is $P_k^{nn'}|(\omega) \longrightarrow \delta_{nn'}F(n)$, where $F(n) \equiv F(p, q) = \langle X_f^{pp}\rangle + \langle X_f^{qq}\rangle$ is the filling factor.

As a result, we obtain the following dispersion equation from the dispersion law for quasiparticles:

$$\det\left\|\delta_{nn'}(\omega - \Omega_n)/F(n) - \tilde{t}_{nn'}(k)\right\| = 0. \qquad (18)$$

This equation resembles in its form the dispersion equation in the tight binding method in the one-electron band theory and differs from it in the following aspects: subscripts $m$ and $n$ number one-particle excitations (quasiparticles) in a multielectron system; local energies $\Omega_n$ now contain intracellular Coulomb interactions rather than one-electron energies; the band structure of quasiparticles depends on the electron concentration (chemical composition), temperature, and external fields via filling factors $F(n)$; and a one-electron model cannot exist for the hard band of quasiparticles.

To determine filling factors $F(n)$ and the position of chemical potential $\mu$, we have to find the self-consistent solution to Eqs. (19) and (20) for the average number of particles in the system $N_e$ and the average values of $X$,

$$N_e = \sum_\sigma \sum_k \int f_F(\omega) A_\sigma(k, \omega) d\omega, \qquad (19)$$

$$\langle X_f^{pp}\rangle = \langle X_f^{pq} X_f^{qp}\rangle = -\frac{1}{\pi}\int f_F(\omega)\langle\langle X_f^{pq}|(X_f^{pq})^\dagger\rangle\rangle, \qquad (20)$$

where $f_F(\omega)$ is the Fermi–Dirac function.

Thus, the LDA + GTB method considers an electron in a strongly correlated system as a linear combination of Hubbard fermions, namely, quasiparticle excitations between various localized multielectron states $d^{n-1}$, $d^n$, $d^{n+1}$ of the electron configurations of a transition-metal ion in the crystal field (Fig. 6). The spectral weight of quasiparticle excitations is determined by the population of multielectron states. With this description, we were able to calculate and analyze the behavior of the band structure of $GdCoO_3$ at a finite temperature. Below, we present the calculation results and the parameters used for the calculations.

At temperature $T = 0$, only the ground term (low-spin singlet $^1A_1$) is populated in $Co^{3+}$ ions in a $GdCoO_3$ crystal. The band structure formed by the transitions (quasiparticle excitations in a multielectron system) $d^6\,{}^1A_1 \longrightarrow d^5\,{}^2T_2\,\tilde{J} = 1/2$, $\tilde{J} = 3/2$ with energies $\Omega_{V1} = E(d^6, {}^1A_1) - E(d^5, {}^2T_2, \tilde{J} = 1/2)$ and $\Omega_{V2} = E(d^6, {}^1A_1) - E(d^5, {}^2T_2, \tilde{J} = 3/2)$ for the valence band and $d^6\,{}^1A_1 \longrightarrow d^7\,{}^2E$ for the conduction band with energies $\Omega_C = E(d^7, {}^2E) - E(d^6, {}^1A_1)$ (Fig. 6, solid lines) has a dielectric gap (Fig. 7a). The transition energies determine the positions of the centers of bands. Obviously, bands $\Omega_V$ and $\Omega_C$ are analogs of the lower and upper Hubbard subbands in the Hubbard model.

When the temperature increases, the quasiparticle spectrum undergoes substantial changes: the thermal population of sublevels $\tilde{J} = 1$ and $\tilde{J} = 2$ of the $^5T_2$ term increases, which results in contributions from possible

transitions not forbidden by the selection rules for spin and spin projection ($\Delta S = \pm 1/2$, $\Delta S_Z = \pm 1/2$). The $d^6$ $^5T_2$ $\tilde{J} = 1$, $\tilde{J} = 2 \longrightarrow d^5\ ^6A_1$ transitions shown as the dashed lines in Fig. 6 with energies $\Omega^*_{V1} = E(d^6, {}^5T_{2g}, \tilde{J} = 1) - E(d^5, {}^6A_1)$ and $\Omega^*_{V2} = E(d^6, {}^5T_{2g}, \tilde{J} = 2) - E(d^5, {}^6A_1)$ are responsible for the appearance of intragap states (excitations $\Omega^*_{V1}$ and $\Omega^*_{V2}$ are higher than $\Omega_{V1}$ and $\Omega_{V2}$ but lower than $\Omega_C$) and for the decrease in the dielectric gap. The results of the self-consistent calculation of the band structure and the position of chemical potential μ(dashed line) for temperature $T = 300$ K are shown in Fig. 7b. The spectral weight and the intragap band width are proportional to the population of sublevels $\tilde{J} = 1$ and 2 of a high-spin state. An increase in the temperature to $T = 300$ K leads to the fact that the bands formed by the transitions $d^6\ ^5T_2\ \tilde{J} = 1$, $\tilde{J} = 2 \longrightarrow d^5\ ^6A_1$ and $d^6\ ^5T_2\ \tilde{J} = 1$, $\tilde{J} = 2 \longrightarrow d^7\ ^4T_1\ \tilde{J} = 1/2$, $\tilde{J} = 3/2$, $\tilde{J} = 5/2$ begin to increase and the dielectric gap decreases. The quasiparticle spectrum and dielectric gap width $E_g$ are seen to be determined by the thermal population of sublevels $\tilde{J} = 1$ and 2 of the $^5T_2$ term in the HS state of the $d^6$ electron configuration of the $Co^{3+}$ ion in the crystal field and, hence, by spin gap $\Delta_{s-t}$. Because of the large spin gap ($\Delta_{s-t} = 2000$ K) in $GdCoO_3$, dielectric gap $E_g$ vanishes as the temperature increases at $T_{IMT} \approx 3000$ K, which is beyond the experimental possibilities and the sample region. In the temperature range 100–600 K, gap $E_g$ is almost temperature independent, $E_g(300) \approx 0.3$ eV.

Below, we present the multielectron Hamiltonian parameters used for the calculations. The hopping integrals for the σ and π bonds were $t^{\sigma}_{pq} = 1.57$ eV, $t^{\pi}_{pq} = 0.84$ eV, and $t_{pp} = 0.5$ eV; the spin–orbit interaction constants were $\lambda(d^5\ ^2T_2) = 160$ K, $\lambda(d^5\ ^4T_1) = 160$ K, $\lambda(d^6\ ^5T_2) = -185$ K, and $\lambda(d^7\ ^4T_1) = -250$ K; the Racah parameters were $A = 1.5$ eV, $B = 0.13$ eV, and $C = 0.55$ eV; and the charge transfer energy was $\Delta_{tr} = 4$ eV.

## 6. CONCLUSIONS

We determined the temperature dependence of the susceptibility of $Co^{3+}$ ions by performing high-temperature measurements of the magnetic susceptibility of $GdCoO_3$ and subtracting the paramagnetic contribution of $Gd^{3+}$ ions. We also calculated this dependence with allowance for the thermal population of high-spin states at the same spin gap.

With the LDA + GTD method, we calculated the band structure of $GdCoO_3$. The energy spectrum of $GdCoO_3$ was found to have intragap states caused by the transitions from the excited high-spin $^5T_2$ state of electron configuration $d^6$ to the high-spin $^6A_1$ ground state of electron configuration $d^5$ of the $Co^{3+}$ ion in the crystal field, and these states were shown to decrease the dielectric gap width with increasing temperature.

## ACKNOWLEDGMENTS

This work was supported by the Ural Branch of the Russian Academy of Sciences and Siberian Branch of the Russian Academy of Sciences (project no. 40), the Russian Foundation for Basic Research (project nos. 09-02-00171-a, 10-02-00251), program 2.3 of the Department of Physical Sciences of Russian Academy of Sciences, and Nonprofit Dinastiya Foundation.

## REFERENCES

1. N. B. Ivanova, S. G. Ovchinnikov, M. M. Korshunov, I. M. Eremin, and N. V. Kazak, Phys.—Usp. **52** (8), 789 (2009).
2. S. Noguchi, S. Kawamata, K. Okuda, H. Nojiri, and M. Motokawa, Phys. Rev. B: Condens. Matter **66**, 094404 (2002).
3. M. Itoh, M. Mori, S. Yamaguchi, and Y. Tokura, Physica B (Amsterdam) **259–261**, 902 (1999).
4. M. Itoh, Y. Tokura, J. Hashimoto, and S. Yamaguchi, Physica B (Amsterdam) **281–282**, 510 (2000).
5. K. Knizek, Z. Jirak, J. Hejtmanek, M. Veverka, M. Marysko, G. Maris, and T. T. M. Palstra, Eur. Phys. J. B **47**, 213 (2005).
6. N. B. Ivanova, J. Bartolome, A. Figueroa, J. Blasco, A. Arauzo, M. S. Platunov, V. V. Rudenko, and N. V. Kazak, Solid State Phenom. **168–169**, 501 (2011).
7. S. G. Ovchinnikov, Yu. S. Orlov, I. A. Nekrasov, and Z. V. Pchelkina, JETP **112** (1), 140 (2011).
8. Y. Tokura, Y. Okimoto, S. Yamaguchi, H. Taniguchi, T. Kimura, and H. Takagi, Phys. Rev. B: Condens. Matter **58**, 1699 (1998).
9. N. B. Ivanova, N. V. Kazak, C. R. Michel, A. D. Balaev, S. G. Ovchinnikov, A. D. Vasil'ev, N. V. Bulina, and E. B. Panchenko, Phys. Solid State **49** (8), 1498 (2007).
10. N. B. Ivanova, N. V. Kazak, C. R. Michel, A. D. Balaev, and S. G. Ovchinnikov, Phys. Solid State **49** (11), 2126 (2007).
11. C. Kittel, *Introduction to Solid State Physics* (Wiley, New York, 1953; Nauka, Moscow, 1978).
12. Z. Ropka and R. J. Radwanski, Phys. Rev. B: Condens. Matter **67**, 172401 (2003).
13. M. J. R. Hoch, S. Nellutla, J. van Tol, E. S. Choi, J. Lu, H. Zheng, and J. F. Mitchell, Phys. Rev. B: Condens. Matter **79**, 214421 (2009).
14. F. J. Birch, Phys. Rev. **71**, 809 (1947).
15. F. J. Birch, J. Geophys. Res. **91**, 4949 (1986).
16. T. Vogt, J. A. Hriljac, N. C. Hyatt, and P. Woodward, Phys. Rev. B: Condens. Matter **67**, 140401(R) (2003).
17. I. S. Lyubutin et al., Nat. Commun. (2011) (in press).

18. M. Tachibana, T. Yoshida, H. Kawaji, T. Atake, and E. Takayama-Muromachi, Phys. Rev. B: Condens. Matter **77**, 094402 (2008).
19. J. Baier, S. Jodlauk, M. Kriener, A. Reichl, C. Zobel, H. Kierspel, A. Freimuth, and T. Lorenz, Phys. Rev. B: Condens. Matter **71**, 014443 (2005).
20. S. Yamaguchi, Y. Okimoto, H. Taniguchi, and Y. Tokura, Phys. Rev. B: Condens. Matter **53**, R2926 (1996).
21. S. Yamaguchi, Y. Okimoto, and Y. Tokura, Phys. Rev. B: Condens. Matter **54**, R11022 (1996).
22. S. G. Ovchinnikov, Sov. Phys. JETP **75** (1), 67 (1992).
23. M. M. Korshunov, V. A. Gavrichkov, S. G. Ovchinnikov, I. A. Nekrasov, Z. V. Pchelkina, and V. I. Anisimov, Phys. Rev. B: Condens. Matter **72**, 165104 (2005).
24. F. C. Zhang and T. M. Rice, Phys. Rev. B: Condens. Matter **37**, 3759 (1988).
25. L. F. Feiner, J. H. Jefferson, and R. Raimondi, Phys. Rev. B: Condens. Matter **53**, 8751(I), 8774(II) (1996).
26. R. O. Zaitsev, Sov. Phys. JETP **43** (3), 574 (1976).
27. V. V. Val'kov and S. G. Ovchinnikov, *Quasiparticles in Strongly Correlated Systems* (Siberian Branch of the Russian Academy of Sciences, Novosibirsk, 2001) [in Russian].
28. Yu. A. Izyumov, M. I. Katsnel'son, and Yu. N. Skryabin, *Magnetism of Itinerant Electrons* (Fizmatgiz, Moscow, 1994) [in Russian].

*Translated by K. Shakhlevich*